A 500-kW PV GENERATOR *I–V* CURVE

Rodrigo Moretón, Eduardo Lorenzo and Javier Muñoz

ABSTRACT

This paper presents the measurement of the *I–V* curve of a 500-kW PV generator by means of an own-made capacitive load. It is shown that *I–V* curve analysis can also be applied to big PV generators and that when measuring the operation conditions with reference modules and taking some precautions (especially regarding the operation cell temperature), it is still a useful tool for characterizing them and therefore can be incorporated into maintenance procedures. As far as we know, this is the largest *I–V* curve measured so far.

KEYWORDS

I–V curve; in-field measurements; quality control; PV generator

1. INTRODUCTION

On-site *I–V* curves of PV generators are a useful tool for assessing not only the effective peak power but also for diagnosing possible performance anomalies (shadows, hot-spots, polarization, connection failures...). Nevertheless, current state of art is restricted to relatively low powers, typically below 100 kW, which is likely due to the practical difficulties of dealing with large currents. In fact, as far as we know, commercial *I–V* tracers are limited to 100 A. Nowadays, however, generators of up to 800 kW are found in PV installations, which implies currents above 1000 A.

This paper presents the *I–V* curve of a 500-kW generator by means of an own-made capacitive load. As far as we know, this is the largest *I–V* curve measured so far. Once obtained, the *I–V* characteristics were extrapolated to standard test conditions (STC) according to IEC-60891 [1] using the incident irradiance, G, and the cell operation temperature, T_C, registered by means of two reference modules.

2. *I–V* CURVE MEASUREMENTS

2.1. The PV generator

The measurement took place in a 2-MW PV plant connected to the grid and located in Lorca (in the South-East of Spain) on the 18 January 2012. This PV plant is formed by four 500-kW generators connected to their respective inverters. Each generator consists of 93 parallel connected strings, each of which is composed of the series connection of 23 monocrystalline silicon modules of 250 W. The nominal values of the PV generator, resulting from the flash-list information given by the manufacturer, are the following: short-circuit current: 810 A; open-circuit voltage: 876 V; and nominal power: 535924 W.

Every inverter had nine bipolar entries, able to accommodate the cables coming from an equal number of DC boxes in the field. These entries were paralleled inside the inverter. The here concerned PV generator included six DC boxes (3 with 15 parallel connected strings and another 3 with 16 parallel connected strings), and therefore, three inverter entries were free. We took advantage of this circumstance by simply connecting our *I–V* tracer to one of these free entries (Figure 1). It is worth noting that in this way, our measurements were made just at the inverter entry. In other words, corresponding results include all the losses until this point (possible early degradation, module mismatching, DC wiring, etc.).

2.2. The *I–V* tracer

We used an up-scaled in-house-made capacitive load based on insulated gate bipolar transistors (IGBTs) that has been described in previous publications [2]. Figure 2 presents a simplified scheme. Key features are the following:

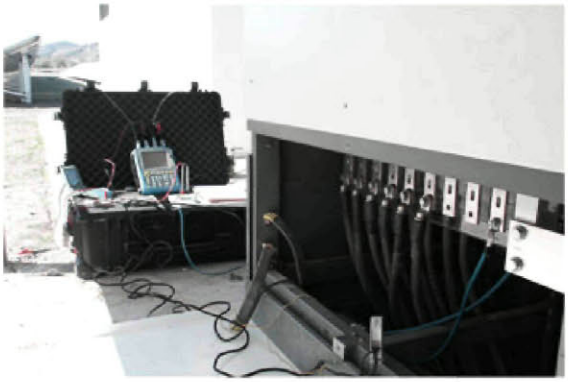

Figure 1. *I–V* tracer connection to the entrance of the inverter, following a four-wire configuration. It can be observed the *I–V* tracer in the background, the six cables from the DC boxes on the right, and the *I–V* tracer connection in a free entry in the foreground.

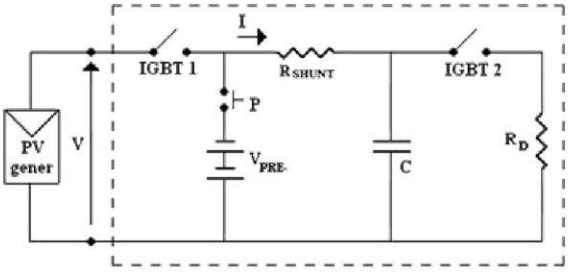

Figure 2. Simplified circuit design. Both insulated gate bipolar transistors (IGBTs) function as switchers, R_D is the capacitors discharge resistance, V_{PRE} the pre-charge battery (acted by switcher P), and C the capacitor.

- An 800-V/16.7-mF capacitor. Roughly, the capacitor charging process is described in terms of a time constant $\tau = RC$, with C being the capacitance and R being the resistance determined by the open-circuit voltage (V_{OC}) and the short-circuit current (I_{SC}) of the generator ($R = V_{OC}/I_{SC}$). Here, $\tau = 18.1$ ms, which leads to charging times of about 30 ms, large enough to avoid transient influences [2].
- A 400-A/1200-V IGBT. In this case, the current measured nearly doubles the limit of the continuous IGBT current (400 A), but because of the very low charging times, it causes no damage to the transistor.
- An 800-A/150-mV 0.5 class (uncertainty of ±0.5%) shunt resistance for measuring the current at the entrance of the load.
- A four-wire connection configuration, with the voltage taken in the connection point, to avoid considering any voltage drop in the *I–V* tracer cables.
- A negative voltage capacitor pre-charge, using a battery, for assuring the capacitor to pass through the short-circuit point. Because of the large current value, there was a voltage loss in the *I–V* tracer cables of about 24 V between the connection point and the entrance to the load. The negative voltage pre-charge compensates this fact allowing the PV generator to pass through the short-circuit point during the charging process.

To minimize the noise/signal relation, we used a four-isolated channel oscilloscope (Metrix Scopix OX7104-c, Chauvin Arnoux, Paris, France) for acquiring the current and voltage signals coming from the generator, and the irradiance and the cell operation temperature coming from the reference modules.

2.3. Measuring conditions

Measuring operation conditions, that is, incident irradiance (G) and cell operation temperature (T_C) that were registered (through I_{SC} and V_{OC}) from two reference modules, previously stabilized and calibrated outdoors at the IES-UPM facilities. The calibration traceability is referred to the CIEMAT. The corresponding uncertainty is ±2.0% in I_{SC}, ±1.0% in V_{OC}, and ±2.5% in P_M. These modules are from the same batches and, therefore, of the same type, as the ones forming the generator. The use of reference modules is the best option when trying to reduce uncertainty associated to spectral, angular, and thermal responses [3–6]. They were installed in the generator's structure in a position free from shadows. Just as a precaution to prevent the uncertainty associated with the effect of dust in the measurements, the reference modules were installed more than 15 days in advance, thus guaranteeing similar dust coverage, as can be observed in Figure 3. In addition, daily rainfalls of more than 6 mm took place in the days previous to the measurement, contributing to clean homogenously all the modules [7,8].

The main uncertainty source when measuring the *I–V* curve of large PV generators on-site is the one associated with the T_C determination [3]. The bigger the generator and the larger the wind speed, the larger the T_C spread among the generator and, therefore, the less representative the value given by a single reference module. To limit the corresponding uncertainty, it is worth assuring the following: charging times of above 20 ms, incident irradiance larger than 800 W/m^2, diffuse/global irradiance proportion

Figure 3. View of the reference modules installation above the generator: there are no appreciable dirtiness differences.

(D/G) lower than 20%, and wind speed lower than 3 m/s. As presented in Table I, in this case, the weather conditions easily fulfilled these requirements. In any case, a thermographic inspection of the installation showed mean temperature differences between the reference module and the modules forming the generator lower than 2 °C.

3. RESULTS

Figure 4 presents the evolution of the current (light line) and the voltage (dark line) during the charging process. As it can be observed, the charging time is greater than 20 ms, which allows to avoid fill factor errors in the measurement [2,9,10]. Despite it is not relevant for the final results, it is interesting to note the acute peak current (≈1400 A), at the beginning of the capacitor charging process. It occurs because of the displacement of majority carriers, inside both p and n zones, required to adapt the length of the depletion zone of the p–n junction to the solar cell applied voltage. Switching the capacitor on implies the PV generator suddenly changing from open-circuit to short-circuit conditions. Hence, the length of the depletion zone must sharply reduce. This process lasts typically for less than 0.2 ms and does not affect the measurement. In fact, it only appears in I–V curves when they are captured with a relatively high sampling frequency. Here, we have used 12.5 kHz. On the other hand, as a precaution to prevent any difference between the voltage reached at the capacitor terminals and the real open-circuit voltage, the latter is also measured just before the charging process.

Once obtained, the curves were extrapolated to STC in accordance with IEC-60891 (procedure 1) using the current and voltage temperature coefficients given by the manufacturer, which are $\alpha = 0.04\%/°\mathrm{K}$ and $\beta = -0.33\%/°\mathrm{K}$, respectively. V_{OC}^{*} and I_{SC}^{*} have been calculated by linear extrapolation from the points around them [1,11]. The series resistance (R_S) was supposed constant through all the operating conditions and estimated assuming a variable fill factor, following the equations proposed by Green [12]. This method has demonstrated a good approximation [13]. The curve correction factor (κ) was fixed at 1.25×10^{-3} Ω/°C, which is a typical value for crystalline silicon cells [14]. Figure 5 shows the I–V curve under real operation conditions (dark line) and once extrapolated to STC (light line). Table I presents the operation conditions and the main characteristics of one of the I–V curves, whereas Table II summarizes the mean values obtained after six measurements. The average maximum power of the PV generator resulted $P_{M,\ IEC\text{-}60891}^{*} = 502761$ W.

Table I. Operation conditions and main results of one of the I–V curves obtained.

			Measured values	Standard test condition values
Location	Lorca (SE of Spain)	I_{SC} [A]	709.0	791.5
Date	18 January 2012	V_{OC} [V]	780.0	846.1
Hour	13:24	I_M [A]	650.0	731.8
G [W/m^2]	899	V_M [V]	614.4	687.6
D [W/m^2]	70	$P_{M,\ IEC\text{-}60891}$ [W]	400550	503216
T_C [°C]	47.2	FF	0.724	0.751
Wind speed [m/s]	<1.5	$P_{M,\ \delta}^{*}$ [W]	400550	495133
Air mass	1.98	κ [Ω/°C]	1.25×10^{-3}	1.25×10^{-3}
t_{CHARGE} [ms]	26.2	R_S [Ω]	0.091	0.071

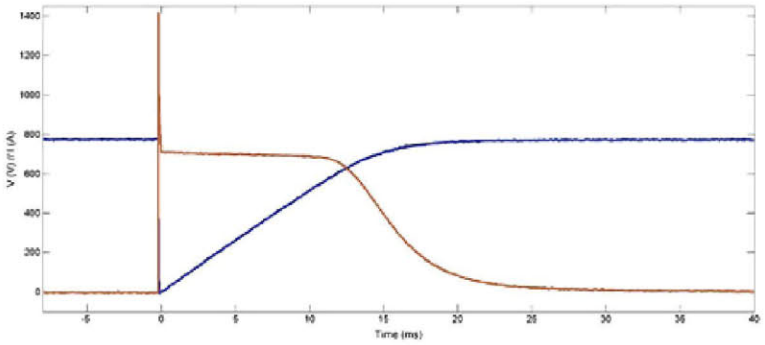

Figure 4. Evolution of I and V during the charging process. The displacement current peak can be observed at $t = 0$.

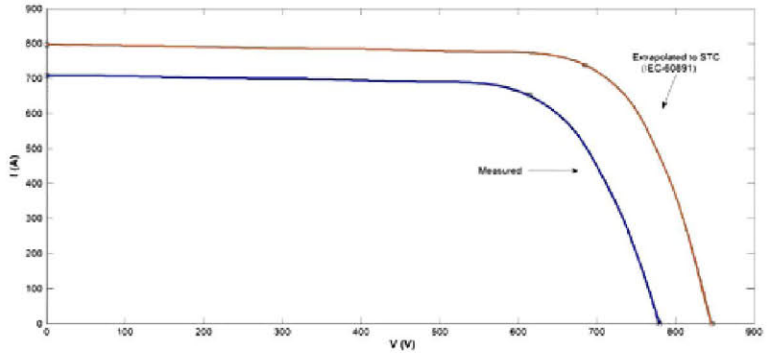

Figure 5. *I–V* curve measured (dark line) and extrapolated to standard test conditions (STC) (light line).

Table II. Mean and standard deviation values of the *I–V* curves obtained.

	Mean ± Δ		
I_{SC}^* [A]	797.2	±	5.1
V_{OC}^* [V]	841.4	±	5.6
I_M^* [A]	737.1	±	13.7
V_M^* [V]	682.1	±	4.9
$P_{M,\ IEC\text{-}60891}^*$ [W]	502761	±	12692
FF^*	0.750	±	0.010
$P_{M,\ \delta}^*$ [W]	492182	±	12497

It is worth mentioning that the uncertainty of the measured power in one curve is lower than 1.4% and the one of the extrapolated power is lower than 3.6%. These values have been calculated following a type B evaluation as established by the "Guide to the Expression of the Uncertainty in Measurement" [15]. The main uncertainty factors have been the calibration of the reference modules and the temperature coefficients [16].

Another way of obtaining the maximum power at STC is to calculate the maximum power from the measured curve and then translate it by using

$$P_M^* = P_M \times \frac{G^*}{G_M} \times \frac{1}{1+\delta(T_C - T^*)}$$

where subscript "M" means measured, superscript "*" means STC, and $\delta = -0.45\%/^\circ K$ is the power temperature coefficient given by the manufacturer [3,17]. Despite its simplicity, there is experimental evidence of this equation being as good as more complex ones [18]. This way, the average maximum power resulted $P_{M,\ \delta}^* = 492182$ W. The difference between both extrapolation methods (2.1%) is small and gives an idea of the uncertainty associated with these procedures and of the coherence of the temperature coefficients.

As it has been presented in previous works, *I–V* curve measurements can be compared with the ones made using a wattmeter [3]. For this PV generator, the analysis with the wattmeter results in an extrapolated maximum power of $P_{M,\ Watt}^* = 501407$ W. The small difference between both procedures (0.3%) indicates coherence and validates the results obtained.

4. CONCLUSIONS

This paper presents the measurement of the *I–V* curve of a 500-kW PV generator by means of an own-made capacitive load. It has been shown that *I–V* curve analysis can also be applied to big PV generators and that, when taking some precautions (especially regarding the T_C), it is still a useful tool for characterizing them and therefore can be incorporated into maintenance procedures.

ACKNOWLEDGEMENTS

The authors would like to acknowledge Gehrlicher Solar, owner of the plant, for giving us the possibility of measuring these curves.

REFERENCES

1. IEC 60891. *Photovoltaic Devices. Procedures for Temperature and Irradiance Corrections to Measure I–V Characteristics*. 2nd edn, International Electrotechnical Commission: Geneva (Switzerland), 2009; ISBN: 2-8318-1073-1.
2. Muñoz J, Lorenzo E. Capacitive load based on IGBTs for on-site characterization of PV arrays. *Solar Energy* 2006; **80**: 1489–1497.
3. Martínez-Moreno F, Lorenzo E, Muñoz J, Moreton R. On the testing of large PV arrays. *Progress in Photovoltaics: Research and applications* 2011. DOI: 10.1002/pip.1102
4. Moreton R., Lorenzo E., Martínez F. Field performance of PV modules quality control process. *23rd*

European Photovoltaic Solar Energy Conference, 2875–2877, Valencia, Spain (2008).
5. Caamaño E, Lorenzo E, Zilles R. Quality control of wide collections of PV modules: lessons learned from the IES experience. *Progress in Photovoltaics: Research and applications* 1999; **7**: 137–149.
6. King DL, Boyson WE, Kratochvil JA. Photovoltaic array performance model. Sandia National Laboratories, Report SAND2004-3535. (2004)
7. García M, Marroyo L., Lorenzo E, Perez M. Soiling and other optical losses in solar-tracking PV plants in Navarra. *Progress in Photovoltaics: Research and Applications* 2010; **19**(2): 211–217. DOI: 10.1002/pip.1004
8. http://eportal.magrama.gob.es/websiar/SeleccionParametrosMap.aspx?dst=1.
9. Blaesser G, Munro D. Guidelines for the assessment of photovoltaic plants. Document C: Initial and periodic tests on photovoltaic plants. Joint Research Centre of the European Communities, Ispra Establishment, Report EUR 16340 EN. (1995).
10. Fabero F, Vela N, Alonso-Abella M, Chenlo F. Characterization of recent commercial technologies of PV modules based on outdoor and indoor I-V curve measurements. 20th European Photovoltaic Solar Energy Conference, 2059–2062, Barcelona, Spain.(2005)
11. Luque A, Hegedus S. *Handbook of Photovoltaic Science and Engineering*. 2nd edn. Chapter 18, Wiley: Hoboken, NJ, USA, 2011; 817–821.
12. Green M. *Solar Cells*. Prentice Hall: Kensigton. Chapter 5, 1982; 95–98.
13. Polverini D, Tzamalis G, Müllejans H. A validation study of photovoltaic module series resistance determination under various operating conditions according to IEC 60891. *Progress in Photovoltaics: Research and Applications* 2012; **20**: 650–660. DOI: 10.1002/pip.1200
14. IEC 60891. *Procedures for Temperature and Irradiance Corrections to Measure I–V Characteristics of Crystalline Silicon Photovoltaic Devices*, 1st edn, International Electrotechnical Commission: Geneva (Switzerland), 1994.
15. ISO/IEC Guide 100:2008. Evaluation of measurement data – Guide to the expression of the uncertainty in measurement. 2008.
16. Makrides G, Zinsser B, Norton M, Georghiou GE, Schubert M, Werner JH. Error sources in outdoor performance evaluation of photovoltaic systems. *24th European Photovoltaic Solar Energy Conference*, 3904–3909, Hamburg, Germany. 2009.
17. Osterwald CR, Translation of device performance measurements to reference conditions. *Solar Cells* 1986; **18**: 269–279.
18. Fuentes M, Nofuentes G, Aguilera J, Talavera DL, Castro M. Application and validation of algebraic methods to predict the behaviour of crystalline silicon PV modules in Mediterranean climates. *Solar Energy* 2007; **81**: 1396–1408. DOI: 10.1016/j.solener.2006.12.008